# Multi-Objective Evolutionary Design of Adenosine Receptor Ligands

Eelke van der Horst,[†,§] Patricia Marqués-Gallego,[†,§] Thea Mulder-Krieger,[†] Jacobus van Veldhoven,[†] Johannes Kruisselbrink,[‡] Alexander Aleman,[‡] Michael T. M. Emmerich,[‡] Johannes Brussee,[†] Andreas Bender,[†] and Adriaan P. IJzerman*,[†]

[†]Division of Medicinal Chemistry, Leiden/Amsterdam Center for Drug Research, P.O. Box 9502, 2300 RA Leiden, The Netherlands
[‡]Leiden Institute of Advanced Computer Science, Leiden University, P.O. Box 9512, 2300RA Leiden, The Netherlands

S *Supporting Information*

ABSTRACT: A novel multiobjective evolutionary algorithm (MOEA) for *de novo* design was developed and applied to the discovery of new adenosine receptor antagonists. This method consists of several iterative cycles of structure generation, evaluation, and selection. We applied an evolutionary algorithm (the so-called Molecule Commander) to generate candidate A_1 adenosine receptor antagonists, which were evaluated against multiple criteria and objectives consisting of high (predicted) affinity and selectivity for the receptor, together with good ADMET properties. A pharmacophore model for the human A_1 adenosine receptor (hA_1AR) was created to serve as an objective function for evolution. In addition, three

support vector machine models based on molecular fingerprints were developed for the other adenosine receptor subtypes (hA_{2A}, hA_{2B}, and hA_3) and applied as negative objective functions, to aim for selectivity. Structures with a higher evolutionary fitness with respect to ADMET and pharmacophore matching scores were selected as input for the next generation and thus developed toward overall fitter ("better") compounds. We finally obtained a collection of 3946 unique compounds from which we derived chemical scaffolds. As a proof-of-principle, six of these templates were selected for actual synthesis and subsequently tested for activity toward all adenosine receptors subtypes. Interestingly, scaffolds **2** and **3** displayed low micromolar affinity for many of the adenosine receptor subtypes. To further investigate our evolutionary design method, we performed systematic modifications on scaffold **3**. These modifications were guided by the substitution patterns as observed in the set of generated compounds that contained scaffold **3**. We found that an increased affinity with appreciable selectivity for hA_1AR over the other adenosine receptor subtypes was achieved through substitution of the scaffold; compound **3a** had a K_i value of 280 nM with approximately 10-fold selectivity with respect to $hA_{2A}R$, while **3g** had a 1.6 μM affinity for hA_1AR with negligible affinity for the hA_{2A}, hA_{2B}, and hA_3 receptor subtypes.
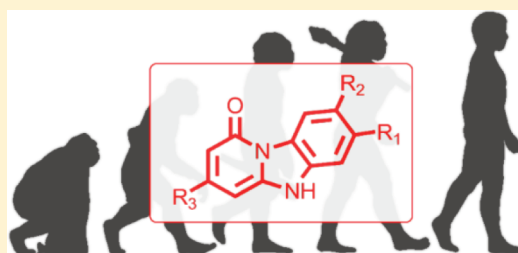
■ INTRODUCTION

Adenosine receptors (AR) belong to the superfamily of G protein-coupled receptors (GPCRs) and are involved in signal transduction.[1,2] To date, four adenosine receptors (AR) have been characterized, the A_1, A_{2A}, A_{2B}, and A_3 subtypes, with adenosine as their endogenous ligand; they are important pharmacological targets in the treatment of different disorders, such as inflammatory, CNS, and cardiovascular diseases.[3] For most subtypes, selective agonists and antagonists have been synthesized, some of which are in clinical stages of development.[4] A_1 AR antagonists are thought to be potentially useful for the treatment of neurological and cardiac disorders, renal failure, and edema; as cognition enhancers; and as antiasthma broncholytic drugs.[5] As for all four adenosine receptors, the human A_1 AR shows a wide distribution over the body with a variety of functions, which may lead to undesired side effects. Therefore, the design and development of A_1AR-selective ligands is an ongoing challenge, where both xanthine and nonxanthine like ligands can be potent and selective A_1 AR antagonists.[4,6]

A core objective of our computational research program is to automate the drug design process as much as possible to present only the most suitable candidates for a biological target to the chemist. Recently, we reported a user-friendly, fully automated desktop application for *de novo* design, the "Molecule Evoluator".[7] An important feature of this software is that, in contrast to many *de novo* design programs, it is an interactive tool for exploring novel chemical structures, while at the same time taking into account the expertise of the medicinal chemists on the fly. This approach has already helped us in designing new molecules active at a number of biogenic amine targets, such as the imidazole and muscarinic (M_{1-5}) receptors, NE and 5-HT transport proteins, and the nicotinic acetylcholine ion channel.[8]

In the present study, we report the development and application of a *de novo* molecule design procedure for the automated generation of new (candidate) lead compounds using multiobjective evolutionary optimization,[9] as imple-

mented in the "Molecule Commander".[10] The consideration of multiple bioactivities, here considered in a multiobjective optimization routine, is important for both achieving the desired efficacy[11] as well as for avoiding off-target effects,[12] and it is in line with current approaches of designing also "selectively unselective"[13] drugs, instead of only hitting single targets thought to be involved in the disease under consideration.

A schematic drawing of the multiobjective evolutionary method is provided in Figure 1, and a detailed description is
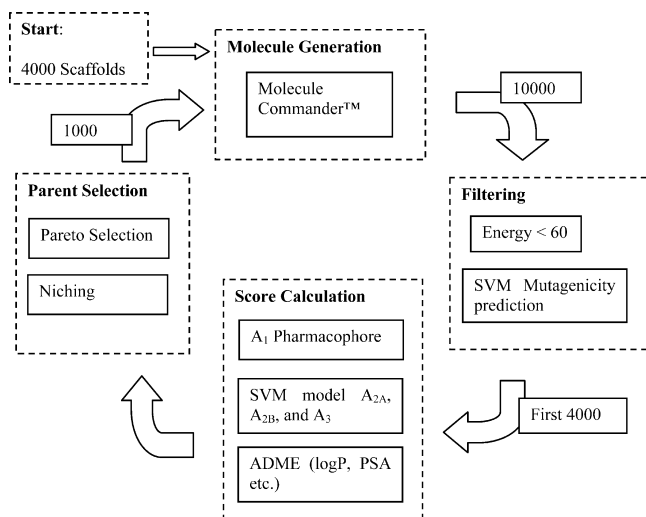
Figure 1. Flowchart of the evolutionary optimization loop (see Experimental Section for a detailed explanation).

reported in the Experimental Section. Our multiobjective evolutionary design procedure consists of an iterative cycle of structure generation, evaluation, and selection of candidate structures. We prospectively validated our methodology toward the design and synthesis of new A_1 AR antagonists, showing that such an approach may indeed yield active and selective ligands for a given target.

■ EXPERIMENTAL SECTION

Reference Ligands. For analysis and model generation, sets of reference ligands for the human adenosine receptor subtypes were retrieved from the ChEMBL database.[14] Query parameters for database retrieval were "Confidence" of 5 or higher (7 being the highest), only direct relationships, and only binding assays. Ligands with pKi values of 5.0 or higher were used, resulting in a set of 633 ligands for A_{2A}, 439 ligands for A_{2B}, and 985 ligands for A_3 human adenosine receptor subtypes. Note that activity type (agonism, antagonism) was not taken into account with compound selection

Initial Input. As input for the first generation of structures, a starting set of 4000 of the most common scaffolds extracted from the purchasable compound set from ZINC (version 8, http://zinc.docking.org, accessed July 2009)[15] was used. Here, a scaffold was defined as the collection of ring atoms and bonds, and linker atoms and bonds connecting these rings.[16,17] Atoms doubly bonded to the scaffold were retained since these often have a major influence on the electronic properties of the scaffold.

Structure Generation. The evolutionary loop (Figure 1) starts by generating new candidate molecules with the Molecule Commander, version 4.2.[10] Like the Molecule Evoluator,[7] this

command-line program creates new structures by randomly modifying or combining a set of input molecular fragments by, e.g., changing atom types, extending or breaking rings, and/or adding small functional groups.

From the set of input structures, the program randomly selects the candidates from which new structures are generated. For each new structure, either a single molecule or a pair of molecules is selected as a starting point for structure generation. When a single molecule is chosen, it will be modified (mutated) to yield a new molecule; when a pair of molecules is chosen, these will be combined into a new molecule. This process is repeated until the desired number of molecules is reached. The same input molecule may be selected several times for the generation of output molecules. For a combination of two molecules, each individual molecule is split into two fragments by breaking bonds and reconnected to a fragment from the other molecule. Fragments are connected using a single bond, which does not lead to the formation of new rings. When generating a new molecule, a maximum of 10 modifications are applied to the same input structure. Simple chemical rules are applied to avoid the generation of improbable structures. In addition, a set of physicochemical properties is calculated on the fly and used to limit the output to structures with desired properties. The program was executed with the following filters enabled: the topological polar surface area[18] was kept between 0 $Å^2$ and 140 $Å^2$, the calculated LogP between −5 and 5, the molecular weight between 200 and 700 Da, hydrogen bond donors between 1 and 5, hydrogen bond acceptors between 1 and 10, rotatable bonds between 0 and 5, and aromatic substituents between 1 and 10. In addition, the NCI Rings filter was enabled without considering the specific (heavy) atom type. This will filter out all structures that contain ring systems that do not occur in the ligand database of the National Cancer Institute (NCI); in this instance, ring systems are compared by shape, not by atom type.

Removal of High-Energy Structures. The occurrence of high-energy structures is a consequence of the random modification of the molecular graph, which may lead to infeasible molecules. Note that until this point, only the topology ("graphs") of the molecules was considered. 3D coordinates were calculated (single conformer) followed by energy minimization, using Pipeline Pilot's "Generate 3D Coordinates" and "Minimize Energy" components, respectively.[19] Energy minimization was performed with default values for all parameters (MaximumNumberOfSteps=1000; ConvergenceEnergyDifference=0.0001). Structures possessing a minimized energy above 60 energy units (arbitrary units) were discarded.

ADMET Prediction. The physicochemical properties for ADME prediction, i.e., the topological Polar Surface Area (PSA), the calculated solubility (LogS), the number of H-bond donors/acceptors, and the molecular weight, were calculated in Pipeline Pilot. Toxicity prediction was limited to the prediction of mutagenicity, which was used as a filter to remove potentially mutagenic compounds. For this, we used a simple categorical Support Vector Machine (SVM) model, which was trained on Ames-test mutagenicity data using ECFP_2 fingerprints (Pipeline Pilot).[20] This served merely as a proof of concept at this stage, and more extensive or proprietary toxicity predictors could readily extend or replace this component.

Optimization Objectives. After the initial generation and filtering phase, the "fittest" molecules were selected to serve as parents for the subsequent generation. To determine which

molecules are "best", several objectives were taken into account, namely high affinity, high selectivity, and good ADME properties. To predict affinity for hA_1 AR, a pharmacophore model was employed that was based on a previously published pharmacophore scheme from our lab for highly potent hA_1 AR antagonists (Supporting Information Figure S1).[21] We chose to replicate this pharmacophore model because it had proved successful for the design of novel ligand chemistry with sufficient selectivity (see Figure 2 for the resulting model).
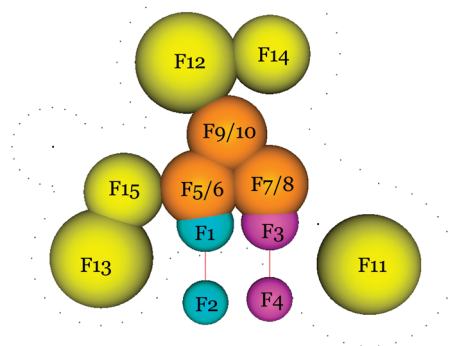
Figure 2. Visual representation of the pharmacophore model used to search for A_1 ligands, based on a previously reported pharmacophore.[21] The aromatic core is represented by three spheres, F5, F7, and F9, and three spheres that indicate the direction of the normal of the aromatic feature, F6, F8, and F10. At least one of the aromatic features with normal projection was demanded to be occupied by a corresponding aromatic feature in the molecule. Three lipophilic regions are represented by spheres F11, F12/F14, and F13/F15. A hydrogen bond acceptor and donor region are represented by F1 and F3, respectively. The direction of the hydrogen bond is indicated with F2 and F4. The gray dots indicate the inclusion volume, the volume into which the molecules generated need to fit for not being subject to a fit penalty.

Pharmacophore Creation. The pharmacophore scheme previously proposed by Chang et al.[21] (Figure S1 of Supporting Information), consisted of an aromatic core surrounded by three lipophilic domains with two hydrogen bond donors and one acceptor, and it had been successfully used to design new adenosine A_1 receptor antagonists. The best compounds from the resulting series have been used in the current study to reconstruct the pharmacophore scheme of Chang et al.,[21] namely, high-affinity compounds N-(2,6-diphenylpyrimidin-4-yl)cyclopentanecarboxamide (LUF5740), N-(2,6-diphenylpyrimidin-4-yl)-2-methylbutanamide (LUF5767), and N-(4,6-diphenylpyrimidin-2-yl)butanamide (LUF5735). The hydrogen atom of the amide bond and the nitrogen of the pyrimidine ring form the hydrogen bond donor and acceptor part. After aligning these features, the aromatic core and lipophilic domains, Lip1, Lip2, and Lip3, were defined. The second hydrogen bond acceptor, corresponding to the carbonyl group in the amidopyrimidines, was omitted since its position and direction could not reliably be derived from the reference compounds. The compounds of the reference set from Chang et al.[21] were used to refine the pharmacophore and further define the included volume. The resulting pharmacophore consisted of 15 features, of which four were marked essential, namely, the hydrogen bond donor and acceptor and corresponding projections (direction) of these features in space. The visual representation of this pharmacophore is

provided in Figure 2. Note that, except for the π-ring normal projections, all features are positioned in one plane.

The pharmacophore score was defined as the number of pharmacophoric features in the molecule that match pharmacophore centers in the model, from which the root-mean-square distance between the feature centers in molecule and pharmacophore was subtracted. A score of zero was assigned to structures with less than eight matches. The score was derived by adding the 1 + negative normalizes RMSD to the number of matching pharmacophore points. The threshold for the features in Figure 2 are as follows: F1 and F3 was 1, for F2 and F4 0.8, for all aromatic features and F14/F15 1.4, and for the lipophilic regions it was 1.8. The number of pharmacophore matches has precedence over the quality of the match.

For pharmacophore creation and compound scoring, Chemical Computing Group's Molecular Operating Environment, version 2008.10 was used.[22]

ADME Score. To predict ADME characteristics, several physicochemical properties, such as solubility (logS), lipophilicity (logP), and polar surface area (PSA), were calculated. Property ranges were defined, outside of which molecules were rejected using filters. Apart from these hard cut-offs, we also included a measure that defined how close a molecule is to ideal property values for ADME. Therefore, between hard cut-offs and ideal property ranges, a gradient was introduced in the ADME score to describe how close the property values are toward the ideal range, giving the algorithm a chance to improve toward good ADME properties. For this, each property was converted to a value between zero and one using a desirability function, where zero (0) indicates undesirable property values and one (1) that property values are excellent. The values of all desirability functions were combined into the desirability index, representing the ADME score. The use of desirability functions/indices originates from areas such as quality control.[23]

SVM Models for Adenosine Receptor Subtypes. In contrast to the pharmacophore model used to predict affinity for the A_1 receptor, a continuous Support Vector Machine (SVM) model[24] trained on ligands of each of the other three adenosine receptor subtypes (A_{2A}, A_{2B}, and A_3) was used to estimate ligand affinity for these receptors. The reason for this is that for the adenosine A_1 receptor the binding features needed to be defined as specifically as possible, while for the other three subtypes (selectivity score) a broad range of possible ligand features had to be detected to ensure selectivity. Three continuous SVM models were trained using Pipeline Pilot ECFP 6 fingerprints for ligands of the human adenosine receptor subtypes A_{2A}, A_{2B}, and A_3. Circular fingerprints of this type have previously been shown to be among the best descriptors capturing molecular features related to bioactivity.[25] Compound training sets were retrieved from ChEMBL (see above). As a background set for training, the Maybridge compound collection included in Pipeline Pilot containing 55 000 compounds was used.

Desirability Indices. The adenosine subtype scores as well as property values were combined into single measures named desirability indices (more specifically, linear Deringer desirability indices), which quantify the level in which individual criteria are met.[26] These indices are calculated as follows: Each property is transformed into a desirability function that expresses how well criteria are met. Desirability functions have a value ranging from zero to one, where zero (0) indicates

that criteria are violated and one (1) that all criteria are entirely satisfied. The function displays a gradual rise between zero and one, the shape of which can vary (linear in this study), to express improvement and to steer evolution toward satisfying the criteria. Desirability functions are either one-sided or two-sided, depending on whether maximization of a value is required or whether the value should be within a specified target range. The individual desirability functions are combined into a desirability index by multiplication. For the subtype desirability index (selectivity), the desirability functions were transformed from the SVM model score for the adenosine receptor subtypes. A SVM model score below 0.2 indicated that affinity was not predicted for the adenosine receptor subtype, resulting in a desirability value of zero, while a score above 0.8 indicated predicted affinity for a subtype, resulting in a desirability value of one. Between 0.2 and 0.8, the value of the desirability function scaled linearly with the SVM model score. These values were then inverted (one minus the desirability value) and combined into the final desirability index that was used as objective. The pharmacophore score represents the number of matching pharmacophore points, which means that an increase of this score translates to improved binding. The score for the model that predicts affinity for the adenosine A_{2A}, A_{2B}, and A_3 receptor subtypes also increases with improved binding; however, this implies decreased selectivity for the adenosine A_1 receptor, and this score should therefore be minimized. For the ADME score, the calculated properties were combined such that an improvement translates to a decreasing score.

Pareto Selection and Niching. A new set of candidates was selected using Pareto selection and niching.[27] Pareto selection is a method to select the set of best solutions of a problem with multiple (conflicting) objectives. The best, or nondominated, solutions are those for which no other solution is superior, for all properties. The nondominated solutions form the Pareto front and have the characteristic that it is not possible to improve on one property without degrading another property. Removing the solutions on the first Pareto front will expose the second Pareto front; removing those will expose the third, etc. The best candidates were then selected and used as input for the next iteration of the evolutionary cycle. Compounds are ranked according to the Pareto front from which they originate. The top-ranked structures represent the best solutions according to all three objectives. However, there are potentially many compounds that share the same Pareto front, for which selection is arbitrary. As a second criterion for the selection, we imposed diversity of the selected molecules. For this, we used dynamic peak identification, or "niching".[28] Niching aims to find a set of clusters, called niches, of the best molecules. Niches are bound areas in descriptor space that are separated by some minimum distance. As a distance measure, we used ECFP_6 fingerprints with the Tanimoto coefficient. Niching starts by selecting an arbitrary molecule from the first Pareto front and assigning it as the first niche center. A second molecule is (randomly) selected from the first Pareto front and is assigned to the first niche if its distance to the niche center is below a predefined minimum; otherwise, it is assigned to a new niche of which it becomes the niche center. The third compound is retrieved from the Pareto front, and its distance to the first niche center is determined. If it is outside the radius of the first niche, the distance to the second niche is determined, to see whether it falls within that niche. If it falls outside all previous niches, it will become the center of a new

niche. This process continues for all subsequent compounds as retrieved from the Pareto ranking, best to worst, by finding a niche they can be assigned to, or creating a new niche. However, the maximum number of compounds per niche is fixed, and upon reaching this number, no new compound members are assigned to it. Other niches may still be accessed though. Since there is also a limit on the number of niches, compounds are eventually discarded when a match is not found. This has the effect of preserving compounds with high Pareto ranking and discarding similar compounds that are already abundant in the set. In addition, it forces the application to preserve diverse parts. This process continues until all molecules are processed or all niches have the maximum number of molecules. When the maximum number of niches and compounds per niche is reached, the remaining compounds are discarded, and the niches collectively serve as input for the next iteration. The general idea behind the niching was to provide a selection of compounds that was independent from the objective space. The settings used in this experiment were a niche radius of 0.85, with a maximum of five molecules per niche and a maximum of 200 niches per generation.

Analysis of Generated Structures. For each generation, the number of known molecules, the occurrence of scaffolds of adenosine receptor ligands, and the number of molecules with a high pharmacophore score were determined. To assess the number of known molecules, presence in ZINC was checked for the generated molecules.

Final Candidate Selection. Generated molecules from all generations were collected, and molecules with a pharmacophore score below 11 were removed. The remaining molecules were grouped by scaffold and ordered by pharmacophore score. To keep only novel candidates for further synthesis, molecules containing ring systems or scaffolds also found in adenosine receptor ligands were removed. For this, ring systems and scaffolds were extracted from the adenosine ligands in ChEMBL (see above). Single rings and fragments without heteroatoms were removed; the rest of the fragments were used for filtering. This final pruning process yielded a collection of novel scaffolds. Subsequently, our chemists searched for possible routes of synthesis and availability of starting materials. Synthesis that required costly or hazardous materials was not considered further. On the basis of ease-of-synthesis, logS, logP, and PSA values, a final set of candidates was selected for synthesis.

Chemistry and Biological Evaluation. To investigate the qualities of the multiobjective evolutionary algorithm, we began with the preparation of suggested candidates. For pragmatic reasons, we chose to first synthesize a set of common scaffolds that were derived from the generated hits. Selecting scaffolds (instead of full structures) for the initial synthesis allowed us to assess the synthetic feasibility and possible activity of a series of generated hits with that scaffold at their core. For scaffolds that proved to be active, these hits would be considered for further synthesis and testing.

The experimental details of the preparation of the selected candidates are provided in subsequent sections of the Supporting Information. Recorded chemical shifts of ^{1}H and ^{13}C NMR spectra and HRMS data and HPLC of each compound are reported.

Affinity for the human adenosine receptor subtypes was determined using radioligand displacement assays. Procedures for these assays are described in the Supporting Information.

■ RESULTS AND DISCUSSION

The three calculated scores—the affinity score, the selectivity score, and the ADMET score—served as input for selecting the best parents for the next generation. This was performed with Pareto selection, which is a method to select the best candidates when considering multiple objectives.[29] In contrast to a simple combination of scores into a single score, Pareto selection considers all three scores simultaneously to select the best candidates. Since evolutionary algorithms have a tendency to focus toward small regions of the chemical search space,[30] diversity of the parent molecules was also taken into account using niching.[27] Niching enforces diversity within populations of candidate solutions by maintaining separated groups, requiring a minimum distance between those groups and a maximum distance between the group members. Distance is based on a (dis)similarity measure such as the Tanimoto index.[31]

For each new generation, the number of known structures, the number of structures with known adenosine ligand scaffolds, and the number of structures with a high pharmacophore score were calculated. When these measures reached a plateau, the process was stopped. Chart 1 shows the

Chart 1. Percentage of Compounds That Contain Known Adenosine Ligand Scaffolds ("Scaffolds") and the Percentage of Compounds with at Least 11, 12, or 13 Pharmacophore Feature Hits ("Hits11"/"Hits12"/"Hits13") per Generation (Number of Generations on *x* Axis)
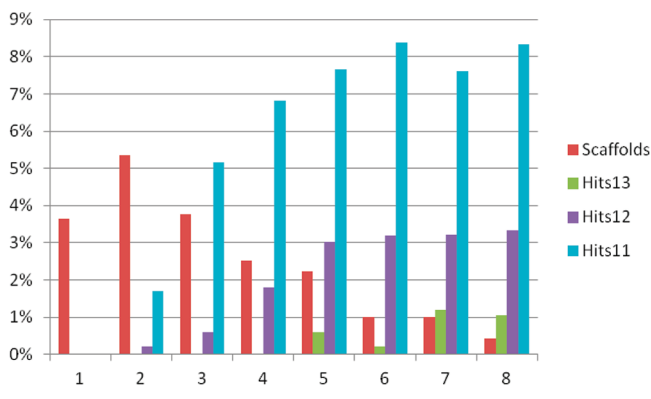
percentage of compounds that contain known adenosine scaffolds as well as those having a high pharmacophore score. The occurrence of scaffolds also found in adenosine ligands (which were removed) gave us some upfront confidence that the generated structures might indeed be potential adenosine receptor ligands. In general, the number of compounds with a high pharmacophore score is expected to improve over the generations while the number of unknown compounds will increase as well. Although generation of novel compounds is preferred from a medicinal chemistry point of view, a high number of unknown compounds also signals for potential difficulties with synthesis planning or acquisition of starting materials. As visualized by the "Scaffolds" bars in Chart 1, the percentage of scaffolds also found in common adenosine receptor ligands decreases with each generation. The data presented in Chart 1 also suggest that the pharmacophore fit improves with each subsequent generation; generated compounds with at least 13 pharmacophore matches first appear in the fifth generation.

The generated molecules from all generations were collected and merged into one set (discarding duplicates), resulting in a set of 3946 unique structures. From this set, structures with a high pharmacophore score, i.e., at least 11 matching pharmacophore points, were selected. The resulting set of 242 hits was examined for novelty by matching the structures against a set of common adenosine receptor scaffolds and ring systems. Forty-three molecules that had a common AR scaffold or ring system at their core were discarded (provided in Table S1 in Supporting Information), yielding a final set of 199 novel candidates. These candidates were grouped by scaffold and ranked according to pharmacophore score, as provided in Table S2 of the Supporting Information, to aid further manual inspection.

As mentioned above, different structures not known to be adenosine receptor ligands were generated and clustered into different groups (i.e., substituted 6:6:5, 6:6:6, or 5:5:6 fused heteroaromatic systems, substituted imidazoles, triazoles, tetrazoles, and quinazolinediones), which demonstrate the variety and diversity of the chemistry provided by our multiobjective evolutionary method (see the Supporting Information, Figure S2). We observed that all of these scaffolds contained substituents of a different nature, at different positions on the scaffold.

Chemistry and Biological Evaluation. From the scaffolds that were derived, six were selected (Figure 2) on the basis of ease of synthesis according to a panel of in-house medicinal chemists. Moreover, we were also interested in the influence of the suggested substituents; therefore, we began with simple substitution (methyl groups) of any on these six scaffolds.

All of these compounds (**1**−**6**) were tested in radioligand binding assays at human A_1 ([^{3}H]DPCPX), A_{2A} ([^{3}H]-ZM241385), A_{2B} ([^{3}H]PSB603[32]), and A_3 receptors ([^{3}H]-PSB11[33] or [^{125}I]AB-MECA). Initially, all compounds were screened at a single concentration of 10 μM on all four receptor subtypes. For compounds that inhibited radioligand binding for more than 25% at one or more receptor subtypes, the K_i values were subsequently determined (Table 1).
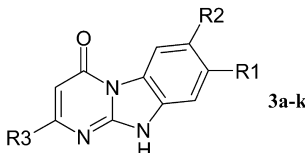
Table 1. Affinities (K_i values) or % Displacement at 10 μM of Compounds 1−6 in Radioligand Binding Assays at Human Adenosine Receptors

compd	$K_i \pm$ SEM (μM, n = 3; or % displacement at 10 μM, average of n = 2)			
	$hA_1{}^a$	$hA_{2A}{}^b$	$hA_{2B}{}^c$	$hA_3{}^d$
1	0%	0%	11%	3%
2	4.6 ± 1.5	4.8 ± 2.3	13%	4%
3	6.2 ± 1.3	1.8 ± 0.3	11 ± 1	0.96 ± 0.17
4	3%	0%	5%	1%
5	13%	−12%	12%	−1%
6	9%	−1%	1%	6%

^{a}Displacement of specific [^{3}H]DPCPX binding from CHO cell membranes expressing human adenosine A_1 receptors or % displacement of specific binding. ^{b}Displacement of specific [^{3}H]ZM241385 binding from HEK 293 cell membranes expressing human adenosine A_{2A} receptors or % displacement of specific binding. ^{c}Displacement of specific [^{3}H]PSB603 binding from CHO cell membranes expressing human adenosine A_{2B} receptors or % displacement of specific binding. ^{d}Displacement of specific [^{3}H]PSB11 binding from CHO cell membranes expressing human adenosine A_3 receptors or % displacement of specific binding.

Table 2. Affinities (K_i Values) or % Displacement at 1 μM of Compounds 3a–3k in Radioligand Binding Assays at Human Adenosine Receptors

R[1] = H, Me

R[2] = H, Me

R[3] = Me, *i*-Pr, Pr, *c*-Hex, Ph, 4-Py

|				$K_i \pm$ SEM (μM, n = 3; or % displacement at 1 μM, average of n = 2)[a]			
compd	R[1]	R[2]	R[3]	hA$_1$[b]	hA$_{2A}$[c]	hA$_{2B}$[d]	hA$_3$[e]
3	H	H	Me	6.2 ± 1.3	1.8 ± 0.3	11 ± 1	0.96 ± 0.17
3a	H	H	*i*-Pr	0.28 ± 0.06	2.4 ± 0.6	19%	−11%
3b	H	H	Pr	1.3 ± 0.3	3.6 ± 0.6	25%	17%
3c	H	H	*c*-Hex	49%	48%	−29%	23%
3d	H	H	Ph	0.13 ± 0.05	43%	0.52 ± 0.18	0.15 ± 0.04
3e	H	H	4-Py	45%	20%	8%	18%
3f	Me	Me	Me	27%	1.7 ± 0.5	−36%	15%
3g	Me	Me	*i*-Pr	1.6 ± 0.5	27%	−21%	11%
3h	Me	Me	Pr	40%	27%	−4%	15%
3i	Me	Me	*c*-Hex	−1%	−5%	−22%	12%
3j	Me	Me	Ph	0.59 ± 0.18	0%	−14%	1.6 ± 0.7
3k	Me	Me	4-Py	10%	0%	*f*	12%

[a]K_i (SEM (n = 3), % displacement (n = 2) at 1 μM. [b]Displacement of specific [^{3}H]DPCPX binding in CHO cells expressing human adenosine A$_1$ receptors or % displacement of specific binding. [c]Displacement of specific [^{3}H]ZM241385 binding in HEK 293 cells expressing human adenosine A$_{2A}$ receptors or % displacement of specific binding. [d]Displacement of specific [^{3}H]PSB603 binding in CHO cells expressing human adenosine A$_{2B}$ receptors or % displacement of specific binding. [e]Displacement of specific [^{125}I]AB-MECA binding in CHO cells expressing human adenosine A$_3$ receptors or % displacement of specific binding. [f]Solubility issues precluded a determination.

As summarized in Table 1, two of the six scaffolds showed activity toward at least two of the adenosine receptor subtypes, including the hA$_1$ AR. Compound 2 had micromolar affinity for both A$_1$ and A$_{2A}$ ARs. Compound 3 appeared active on all four adenosine receptor subtypes, also in the micromolar range. We were satisfied with the 33% "hit rate", although A$_1$ receptor selectivity could not be detected for these scaffolds. However, each of these bare scaffolds represented a series of generated compounds that consisted of this particular scaffold with various substituents attached. Exploring the substitution patterns was anticipated to result in more selective compounds, as was already suggested by the selectivity score of these generated compounds.

Instead of exactly replicating generated hits, which would prove synthetically demanding, we analyzed for each scaffold substitution patterns found in generated hits in which the scaffold was present, in order to identify common areas and substituent types for substitution. As a next step, we decided therefore to perform a systematic modification by substitution of the novel 6:5:6-fused scaffold 3 to investigate a possible enhancement of affinity and subtype selectivity for the hA$_1$AR.

Inspection of the generated molecules that contained this 10H-pyrimido-[1,2-a]-benzimidazol-4-one scaffold revealed that the insertion of a simple alkyl chain at the R3 position of the scaffold led to high-scoring molecules. Therefore, we replaced the methyl group on scaffold 3 with different alkyl groups (Figure 2) and investigated the influence thereof on adenosine receptor affinity. A series of compounds was synthesized (3a–3k) by reacting the corresponding 2-aminobenzimidazole with the appropriate β-keto-ester under microwave conditions (see the Supporting Information). All derivatives were tested in radioligand binding studies starting at either 10 μM or 1 μM concentrations on the A$_1$ AR. To determine the selectivity of these derivatives for the A$_1$ AR, the

interaction with the other AR subtypes (A$_{2A}$, A$_{2B}$, and A$_3$) was also investigated. For those derivatives that gave more than 50% displacement at 1 μM concentration, whole displacement curves were recorded to determine the K_i value of each compound. In Table 2, both % displacement and K_i values for each derivative are summarized.
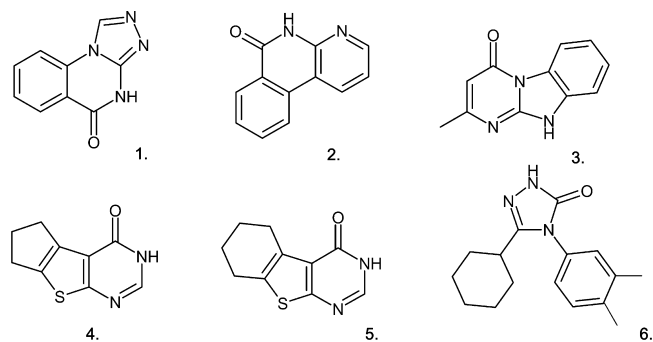

Figure 3. Chemical structures of selected scaffolds generated using the multiobjective evolutionary design method: [1,2,4]triazolo[4,3-a]-quinazolin-5-one (1), 4-aza-5[H]-phenanthridin-6-one (2), 2-methylpyrimido[1,2-a]benzimidazol-4(10H)-one (3), 3,5,6,7-tetrahydro-4H-cyclopenta[4,5]thieno[2,3-d]pyrimidin-4-one (4), 5,6,7,8-tetrahydro[1]benzothieno[2,3-d]pyrimidin-4(3H)-one (5), and 5-cyclohexyl-4-(3,4-dimethylphenyl)-2,4-dihydro-3H-1,2,4-triazol-3-one (6).

We observed that increasing bulkiness by introducing an iso-propyl group at the R3 position (3a) yielded improved affinity on the hA$_1$ AR, with a K_i value of 0.28 ± 0.06 μM, 22-fold lower than the K_i value of parent scaffold 3 (Table 2), and also better selectivity toward the other AR subtypes. An n-propyl group at the R3 position (3b) also improved the K_i value compared to compound 3 but less so than the iso-propyl

substituent. These findings prompted us to synthesize the cyclohexyl derivative **3c**, which provides an even bulkier substituent at the R3 position, yet not aromatic. Although not elaborated further, **3c** showed 49% displacement at 1 μM on the hA$_1$ AR, suggesting a K_i value in the low micromolar region, similar to that found for the propyl derivative **3b**. Subsequently, aromatic rings were also explored as substituents at the R3 position, introducing an additional planar lipophilic domain on the structure. As listed in Table 2, inserting a phenyl ring at the R3 position led to compound **3d** with highest affinity on the A$_1$ receptor, with a K_i value of 0.13 $\pm$ 0.05 μM, although selectivity was lost toward both hA$_{2B}$ and hA$_3$ AR. 4-Pyridyl substitution in **3e** led to a less active compound (43% displacement of [^{3}H]DPCPX radioligand binding at 1 μM).

Modifications on both R1 and R2 positions on the 10H-pyrimido-[1,2-a]-benzimidazole-4-one scaffold were also investigated. Introducing methyl groups on both R1 and R2 positions decreased interaction with the adenosine receptors (Table 2). A pronounced example of this observation is compound **3g** compared to its analogue **3a**, displaying an almost 6-fold lower affinity for the hA$_1$ AR. Compound **3g** had negligible affinity for the other adenosine receptor subtypes with low % displacement on A$_{2A}$, A$_{2B}$, and A$_3$ AR at 1 μM concentration (27%, −21%, and 11%, respectively). Therefore, the combination of R3 = *i*-Pr and R1 = R2 = Me yielded the most selective compound of this series. Interestingly, compound **3g** had also high resemblance to an equivalent hit (Figure 4) from the de novo design procedure, indicative of the predictive power of the method.
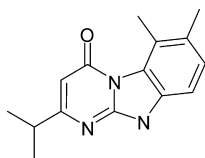
Figure 4. Source compound from the generated hits (Table S2, Supporting Information) that has a high resemblance to compound **3g**. The structures differ with respect to the position of a methyl group on the phenyl ring.

The closest analogues of scaffold **3** reported in the literature are the so-called ATBIs developed by Da Settimo and colleagues.[34] Their general structure and some representative examples (comparable to **3d** and **3j**) with their K_i values at the hA$_1$ AR[35] are in Figure 5. They are also active in the submicromolar range, suggesting that the adenosine A$_1$ receptor tolerates subtle changes in the central scaffold.

The rationale of deriving scaffolds from the generated hits was to condense the many suggested candidates to a comprehensible list that could be discussed with our medicinal chemists. For each scaffold, we also compiled substituent tables, to get a general impression where scaffolds should be extended and with what type of substituent/functional group. Starting
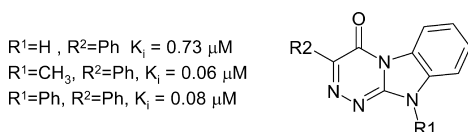
synthesis with a common scaffold was seen as logical since these represented a range of generated hits (i.e., similar derivatives) with a similar synthetic route. Exploring the synthetic feasibility of the scaffold allowed us to assess the feasibility of all its derivatives that existed in the set of generated compounds. Most importantly, synthesizing a scaffold would hint at the potential activity of the parent structures from which it was derived. Would we have chosen to start with the synthesis of complete, i.e., unchanged, structures as generated by our method, we would have risked testing derivatives for which the scaffold was active but the derivative not due to unfavorable placement of its substituents. This is similar to the rationale behind fragment-based drug discovery, that is, to initially screen for low molecular weight compounds which display some affinity that are then used as starting points to find more complex molecules with high affinity. As was shown for compound **3g** (which is a nearly exact match of its equivalent structure in the generated compound set, except for a methyl substituent), suggested compounds have higher affinity and display selectivity.

■ CONCLUSIONS

We developed a de novo multiobjective evolutionary design procedure and applied it to adenosine receptors, a subclass of the superfamily of G protein-coupled receptors. This method provides the user with a fast and automated generation of best candidate structures and close analogues thereof. Significant micromolar affinity was obtained with two (out of six) scaffolds that were generated in the design process, 4.6 and 4.8 μM for respectively hA$_1$AR and hA$_{2A}$AR for scaffold **2** and 6.2, 1.8, 11, and 0.96 μM for respectively hA$_1$AR, hA$_{2A}$AR, hA$_{2B}$AR, and hA$_3$AR for scaffold **3**, showing its versatility and relatively high "hit rate". Moreover, by reintroducing some of the original substituents as observed in the generated compounds which had scaffold **3** at their core, affinity and selectivity toward the A$_1$ adenosine receptor was improved. For instance, the compound with highest selectivity for hA$_1$AR (**3g**) had a 1.6 μM affinity for this receptor and displayed little displacement at the hA$_{2A}$, hA$_{2B}$, and hA$_3$ receptor subtypes. In more general terms, an automated design strategy that optimizes multiple parameters simultaneously appeared feasible and attractive as it allows an unbiased exploration of chemical space. We anticipate that novel scaffolds for other targets can be derived in a similar way, thus helping the medicinal chemists in their drug discovery efforts.

■ ASSOCIATED CONTENT

⑤ Supporting Information

List of chemical structures generated using our multiobjective evolutionary method, schematic diagram of pharmacophore proposed by Chang et al.,[21] synthetic routes and schemes for all the compounds described in this paper, **1−6** and **3a−3k**, the experimental details of their synthesis and ^{1}H NMR and ^{13}C NMR spectroscopic data, HRMS data and HPLC data. This material is available free of charge via the Internet at http://pubs.acs.org.

R^1=H , R^2=Ph K_i = 0.73 μM
R^1=CH$_3$, R^2=Ph, K_i = 0.06 μM
R^1=Ph, R^2=Ph, K_i = 0.08 μM

Figure 5. Aryltriazinobenzimidazolones (ATBIs) developed by Da Settimo and colleagues.[34,35]

■ AUTHOR INFORMATION

Corresponding Author

*Tel.: +31-71-5274651. Fax: +31-71-5274565. E-mail: ijzerman@lacdr.leidenuniv.nl.

■ **REFERENCES**
(1) Fredholm, B. B.; IJzerman, A. P.; Jacobson, K. A.; Klotz, K. N.; Linden, J. International Union of Pharmacology. XXV. Nomenclature and classification of adenosine receptors. *Pharmacol. Rev.* **2001**, *53*, 527−552.
(2) Ralevic, V.; Burnstock, G. Receptors for purines and pyrimidines. *Pharmacol. Rev.* **1998**, *50*, 413−492.
(3) Jacobson, K. A.; Gao, Z. G. Adenosine receptors as therapeutic targets. *Nat. Rev. Drug Discovery* **2006**, *5*, 247−264.
(4) Muller, C. E.; Jacobson, K. A. Recent developments in adenosine receptor ligands and their potential as novel drugs. *Biochim. Biophys. Acta, Biomembr.* **2011**, *1808*, 1290−1308.
(5) Muller, C. E. A(1)-adenosine receptor antagonists. *Expert Opin. Ther. Pat.* **1997**, *7*, 419−440.
(6) Baraldi, P. G.; Tabrizi, M. A.; Gessi, S.; Borea, P. A. Adenosine receptor antagonists: Translating medicinal chemistry and pharmacology into clinical utility. *Chem. Rev.* **2008**, *108*, 238−263.
(7) Lameijer, E. W.; Kok, J. N.; Bäck, T.; IJzerman, A. P. The Molecule Evoluator. An Interactive Evolutionary Algorithm for the Design of Drug-Like Molecules. *J. Chem. Inf. Model.* **2006**, *46*, 545−552.
(8) Lameijer, E. W.; Tromp, R. A.; Spanjersberg, R. F.; Brussee, J.; IJzerman, A. P. Designing active template molecules by combining computational de novo design and human chemist's expertise. *J. Med. Chem.* **2007**, *50*, 1925−1932.
(9) Nicolaou, C. A.; Brown, N.; Pattichis, C. S. Molecular optimization using computational multi-objective methods. *Curr. Opin. Drug Discovery Dev.* **2007**, *10*, 316−324.
(10) *Molecule Commander*, version 4.2; Cidrux Pharminformatics B.V.: Haarlem, The Netherlands.
(11) Bender, A.; Young, D. W.; Jenkins, J. L.; Serrano, M.; Mikhailov, D.; Clemons, P. A.; Davies, J. W. Chemogenomic data analysis: Prediction of small-molecule targets and the advent of biological fingerprints. *Comb. Chem. High Throughput Screening* **2007**, *10*, 719−731.
(12) Bender, A.; Scheiber, J.; Glick, M.; Davies, J. W.; Azzaoui, K.; Hamon, J.; Urban, L.; Whitebread, S.; Jenkins, J. L. Analysis of Pharmacology Data and the Prediction of Adverse Drug Reactions and Off-Target Effects from Chemical Structure. *ChemMedChem* **2007**, *2*, 861−873.
(13) Morphy, R.; Kay, C.; Rankovic, Z. From magic bullets to designed multiple ligands. *Drug Discovery Today* **2004**, *9*, 641−651.
(14) de Matos, P.; Alcantara, R.; Dekker, A.; Ennis, M.; Hastings, J.; Haug, K.; Spiteri, I.; Turner, S.; Steinbeck, C. Chemical Entities of Biological Interest: an update. *Nucleic Acids Res.* **2010**, *38*, D249−254.
(15) Irwin, J. J.; Shoichet, B. K. ZINC-A Free Database of Commercially Available Compounds for Virtual Screening. *J. Chem. Inf. Model.* **2005**, *45*, 177−182.
(16) Bemis, G. W.; Murcko, M. A. The Properties of Known Drugs. 1. Molecular Frameworks. *J. Med. Chem.* **1996**, *39*, 2887−2893.

(17) Bemis, G. W.; Murcko, M. A. Properties of Known Drugs. 2. Side Chains. *J. Med. Chem.* **1999**, *42*, 5095−5099.
(18) Ertl, P.; Rohde, B.; Selzer, P. Fast Calculation of Molecular Polar Surface Area as a Sum of Fragment-Based Contributions and Its Application to the Prediction of Drug Transport Properties. *J. Med. Chem.* **2000**, *43*, 3714−3717.
(19) *Scitegic Pipeline Pilot*, 6.1.5.0 Student ed.; Accelrys, Inc.: San Diego, CA, 2007.
(20) Kazius, J.; McGuire, R.; Bursi, R. Derivation and Validation of Toxicophores for Mutagenicity Prediction. *J. Med. Chem.* **2005**, *48*, 312−320.
(21) Chang, L. C. W.; Spanjersberg, R. F.; Kunzel, J. K. V.; Mulder-Krieger, T.; van den Hout, G.; Beukers, M. W.; Brussee, J.; IJzerman, A. P. 2,4,6-trisubstituted pyrimidines as a new class of selective adenosine A(1) receptor antagonists. *J. Med. Chem.* **2004**, *47*, 6529−6540.
(22) *Molecular Operating Environment*, 2008.10; Chemical Computing Group: Montreal, Quebec, Canada, 2008.
(23) Trautmann, H.; Weihs, C. On the distribution of the desirability index using Harrington's desirability function. *Metrika* **2006**, *63*, 207−213.
(24) Ivanciuc, O. Applications of Support Vector Machines in Chemistry. *Rev. Comput. Chem.* **2007**, *23*, 291−400.
(25) Bender, A.; Jenkins, J. L.; Scheiber, J.; Sukuru, S. C. K.; Glick, M.; Davies, J. W. How Similar Are Similarity Searching Methods? A Principal Component Analysis of Molecular Descriptor Space. *J. Chem. Inf. Model.* **2009**, *49*, 108−119.
(26) Kruisselbrink, J. W.; Emmerich, M. T. M.; Bäck, T.; Bender, A.; IJzerman, A. P.; van der Horst, E. Combining Aggregation with Pareto Optimization: A Case Study in Evolutionary Molecular Design. In *Evolutionary Multi-Criterion Optimization*; Springer-Verlag: Berlin/Heidelberg, 2009; Vol. *5467*, pp 453−467.
(27) Kruisselbrink, J. W.; Aleman, A.; Emmerich, M. T. M.; IJzerman, A. P.; Bender, A.; Bäck, T.; van der Horst, E. Enhancing search space diversity in multi-objective evolutionary drug molecule design using niching. In *Proceedings of the 11th Annual conference on Genetic and evolutionary computation*, Montreal, Québec, Canada, 2009; ACM: New York, 2009; pp 217−224.
(28) Shir, O.; Preuss, M.; Naujoks, B.; Emmerich, M. Enhancing Decision Space Diversity in Evolutionary Multiobjective Algorithms. In *Proceedings of the 5th International Conference on Evolutionary Multi-Criterion Optimization*, Nantes, France, 2009; Springer: Berlin/Heidelberg, 2009; pp 95−109.
(29) Nicolaou, C. A.; Apostolakis, J.; Pattichis, C. S. De Novo Drug Design Using Multiobjective Evolutionary Graphs. *J. Chem. Inf. Model.* **2009**, *49*, 295−307.
(30) Preuss, M.; Schönemann, L.; Emmerich, M. Counteracting genetic drift and disruptive recombination in (μpluskommaλ)-EA on multimodal fitness landscapes. In *Proceedings of the 2005 conference on Genetic and evolutionary computation*; ACM: Washington, DC, 2005; pp 865−872.
(31) Bender, A.; Glen, R. C. Molecular similarity: a key technique in molecular informatics. *Org. Biomol. Chem.* **2004**, *2*, 3204−3218.
(32) Borrmann, T.; Hinz, S.; Lertarelli, D. C. G.; Li, W. J.; Florin, N. C.; Scheiff, A. B.; Muller, C. E. 1-Alkyl-8-(piperazine-1-sulfonyl)-phenylxanthines: Development and Characterization of Adenosine A(2B) Receptor Antagonists and a New Radioligand with Sub-nanomolar Affinity and Subtype Specificity. *J. Med. Chem.* **2009**, *52*, 3994−4006.
(33) Muller, C. E.; Diekmann, M.; Thorand, M.; Ozola, V. [H-3]8-ethyl-4-methyl-2-phenyl-(8R)-4,5,7,8-tetrahydro-1H-imidazo[2,1-i]-purin-5-one ([H-3]PSB-11), a novel high-affinity antagonist radioligand for human A(3) adenosine receptors. *Bioorg. Med. Chem. Lett.* **2002**, *12*, 501−503.
(34) Da Settimo, F.; Primofiore, G.; Taliani, S.; Marini, A. M.; La Motta, C.; Novellino, E.; Greco, G.; Lavecchia, A.; Trincavelli, L.; Martini, C. 3-Aryl[1,2,4]triazino[4,3-a]benzimidazol-4(10H)-ones: A New Class of Selective A1 Adenosine Receptor Antagonists. *J. Med. Chem.* **2001**, *44*, 316−327.

(35) Da Settimo, F.; Primofiore, G.; Taliani, S.; La Motta, C.; Novellino, E.; Greco, G.; Lavecchia, A.; Cosimelli, B.; Iadanza, M.; Klotz, K.-N.; Tuscano, D.; Trincavelli, M. L.; Martini, C. A1 adenosine receptor antagonists, 3-aryl[1,2,4]triazino[4,3-a]benzimidazol-4-(10H)-ones (ATBIs) and N-alkyl and N-acyl-(7-substituted-2-phenylimidazo[1,2-a][1,3,5]triazin-4-yl)amines (ITAs): Different recognition of bovine and human binding sites. *Drug Dev. Res.* **2004**, *63*, 1−7.

1721

dx.doi.org/10.1021/ci2005115 | *J. Chem. Inf. Model.* 2012, 52, 1713−1721